

## DNA Damage and DNA Damage Responses in THP-1 Monocytes after Exposure to Spores of either *Stachybotrys chartarum* or *Aspergillus versicolor* or to T-2 toxin

Kirsten E. Rakkestad,\* Ida Skaar,† Vibeke E. Ansteinsson,‡¶ Anita Solhaug,† Jørn A. Holme,\* James J. Pestka,§ Jan T. Samuelsen,¶ Hans J. Dahlman,\* Jan K. Hongslo,\* and Rune Becher\*,<sup>1</sup>

\*Department of Air Pollution and Noise, Division of Environmental Medicine, Norwegian Institute of Public Health, N-0403 Oslo, Norway; †Department of Feed and Food Safety, National Veterinary Institute, N-0106 Oslo, Norway; ‡Department of Clinical Dentistry-Biomaterials, University of Bergen, N-5009 Bergen, Norway; §Department of Microbiology and Molecular Genetics, Michigan State University, East Lansing, Michigan 48824; and ¶NIOM—Nordic Institute of Dental Materials, N-1305 Haslum, Norway

<sup>1</sup> To whom correspondence should be addressed at Department of Air Pollution and Noise, Division of Environmental Medicine, Norwegian Institute of Public Health, PO Box 4404, Nydalen, N-0403 Oslo, Norway. E-mail: rune.becher@fhi.no.

Received October 16, 2009; accepted January 31, 2010

We have characterized cell death in THP-1 cells after exposure to heat-treated spores from satratoxin G-producing *Stachybotrys chartarum* isolate IBT 9631, atranone-producing *S. chartarum* isolate IBT 9634, and sterigmatocystin-producing *Aspergillus versicolor* isolate IBT 3781, as well as the trichothecenes T-2 and satratoxin G. Spores induced cell death within 3–6 h, with *Stachybotrys* appearing most potent. IBT 9631 induced both apoptosis and necrosis, while IBT 9634 and IBT 3781 induced mostly necrosis. T-2 toxin and satratoxin G caused mainly apoptosis. Comet assay ± formamidopyrimidine DNA glycosylase showed that only the spore exposures induced early (3h) oxidative DNA damage. Likewise, only the spores increased the formation of reactive oxygen species (ROS), suggesting that spores as particles may induce ROS formation and oxidative DNA damage. Increased Ataxia Telangiectasia Mutated (ATM) phosphorylation, indicating DNA damage, was observed after all exposures. The DNA damage response induced by IBT 9631 as well as satratoxin G was characterized by rapid (15 min) activation of p38 and H2AX. The p38 inhibitor SB 202190 reduced IBT 9631-induced H2AX activation. Both IBT 9631 and T-2 induced activation of Chk2 and H2AX after 3 h. The ATM inhibitor KU 55933, as well as transfection of cells with ATM siRNA, reduced this activation, suggesting a partial role for ATM as upstream activator for Chk2 and H2AX. In conclusion, activation of Chk2 and H2AX correlated with spore- and toxin-induced apoptosis. For IBT 9631 and satratoxin G, additional factors may be involved in triggering apoptosis, most notably p38 activation.

**Key Words:** mold; mycotoxins; DNA damage response; apoptosis.

Mold spores and their associated mycotoxins have been suggested to be the cause of a variety of human health problems such as asthma and allergic rhinitis related to water-

damaged indoor environments. Animal studies have shown that mycotoxins may cause a variety of adverse effects, including acute toxic effects and cancer (Etel, 2002). In the lung, inhaled mycotoxins may exert their effects through direct cytotoxicity as well as induction of inflammatory responses. However, linking adverse human health effects other than allergic responses to molds and mycotoxins in the indoor environment is still highly controversial (Hardin *et al.*, 2003). Furthermore, inflammagenic substances other than mycotoxins can be present within spores (Green *et al.*, 2005) and might potentially contribute to their suggested health effects. Thus, it is particularly important to understand how spores of toxigenic molds affect the innate immunoresponse. An important issue to further explore in this context is the more specific mechanisms involved in the effects of various mycotoxins versus the effect of spores *per se*.

*Stachybotrys chartarum* is a mold that is frequently associated with water-damaged indoor environments and reported complaints about poor indoor air quality. Many *S. chartarum* isolates produce trichothecenes, a large family of highly toxic mycotoxins. Trichothecenes might contribute to immune dysfunction, impaired respiratory function, as well as neuronal cell death. The trichothecenes are often divided into several groups according to both their chemical properties and their producer fungi. The macrocyclic trichothecenes, which include the satratoxins, are produced by several fungal species including *Stachybotrys* spp., whereas T-2 toxin, a type A trichothecene, is synthesized by various *Fusarium* molds. In addition to trichothecenes, *S. chartarum* can also produce a family of mycotoxins known as atranones that are able to induce pulmonary inflammation in animals (Pestka *et al.*, 2008).

Another mold frequently associated with indoor air quality problems is the *Aspergillus*. More than 200 *Aspergillus* species

are known that can produce a wide variety of mycotoxins. Among these is the sterigmatocystin-producing *Aspergillus versicolor*. Sterigmatocystin has been identified in samples of carpet dust (containing *A. versicolor* isolates) from damp indoor environments (Engelhart *et al.*, 2002). Sterigmatocystin is a biosynthetic precursor of aflatoxins and is considered to be a potent carcinogen, mutagen, and teratogen (Versilovskis and De Saeger, 2010).

It has been suggested that the most prominent effect of trichothecenes is their action as potent inhibitors of protein synthesis (Cole and Cox, 1981; McLaughlin *et al.*, 1977). Trichothecenes also have inhibitory effects on RNA and DNA synthesis, but this is most likely secondary to the inhibition of protein synthesis (Cundliffe and Davies, 1977; Nagase *et al.*, 2002; Nielsen *et al.*, 2002; Yang *et al.*, 2000). A number of studies have demonstrated the capability of trichothecenes to induce apoptotic cell death in a variety of cell types (Islam *et al.*, 2008; Shifrin and Anderson, 1999; Yang *et al.*, 2000). Inhibitors of protein synthesis as such have been reported to both increase and inhibit apoptosis depending on cell-stimuli combination (Mattson and Furukawa, 1997; Olmo *et al.*, 2001); thus, there is no generalizable link between translational inhibition and apoptosis. Recently, trichothecenes were reported to induce apoptosis through activation of mitogen-activated protein kinase (MAPK) via a mechanism that has been termed the ribotoxic stress response. Data from Zhou *et al.* (2003) suggest that double-stranded RNA-activated protein kinase R (PKR) is a critical upstream mediator of the ribotoxic stress response induced by the trichothecene deoxynivalenol (DON). Furthermore, satratoxin G-induced apoptosis in PC-12 neuronal cells was found to be mediated by PKR. Other apoptosis-triggering signals that could be relevant for the molds includes endoplasmic reticulum stress and DNA damage.

Ruotsalainen *et al.* (1998) found that *in vitro* exposure to *Stachybotrys* spp. spores resulted in an immediate increase in reactive oxygen species (ROS) formation in human polymorphonuclear leukocytes, which thereby may result in oxidative DNA damage. Theoretically, this effect could be due to the spore being a particle, as particles are known to induce oxidative damage (González-Flecha, 2004). Another possibility could be that the spore-associated mycotoxins might induce the observed DNA damage. *Stachybotrys chartarum* extracts have been shown to oxidize glutathione, induce DNA single strand breaks, as well as increase the frequency of micronuclei (Wang and Yadav, 2006). Very recently, T-2 toxin was suggested to cause oxidative damage, DNA damage, and phosphorylation of p53 as early as 2–4 h after start of exposure (Chaudhari *et al.*, 2009). Furthermore, sterigmatocystin, which is structurally related to the aflatoxins, although considered less potent, is known to form DNA adducts (Gopalakrishnan *et al.*, 1992).

The cellular response to DNA damage involves pathways important for cell survival reactions, including regulation of

DNA repair, DNA replication, and proliferation. If the amount or type of damage exceeds the repair capacity of the cells, the apoptotic process may be triggered (Roos and Kaina, 2006). One important sensor of DNA damage is Ataxia Telangiectasia Mutated (ATM) kinase, a member of the phosphoinositide 3-kinase (PI3K) cell signaling family, often triggered by double-stranded DNA breaks (DSBs) and larger topological changes (Burma *et al.*, 2001; Lee and Paull, 2005, 2007). Downstream target molecules of ATM kinase include the checkpoint kinase Chk2 and the histone H2AX. Chk2 is thought to play a central role in the DNA damage response by relaying signals to the cell cycle machinery. This may result in a delayed cell cycle allowing repair of DNA damage or in cell death if repair cannot take place. Another step in an efficient recognition and repair response to DSB is the phosphorylation of H2AX to  $\gamma$ H2AX. While several members of the PI3K-like family of protein kinases including DNA-protein kinase, ATM, and ATR (ATM and Rad3 related) as well as the MAPK p38 have been implicated in H2AX phosphorylation, recent findings suggest that ATM is the major kinase involved in this phosphorylation (Burma *et al.*, 2001).

The aim of this study was to compare how spores from different toxigenic molds affect the monocyte-macrophage lineage, a critical element of the innate immune response. We characterized mechanisms of cell death in the THP-1 monocyte model after exposure to heat-treated non-viable spores from trichothecene-producing *S. chartarum* (IBT 9631), atranone-producing *S. chartarum* (IBT 9634), or sterigmatocystin-producing *A. versicolor* (IBT 3781) strains. More specifically, the IBT 9631-induced apoptosis was compared with the effects of the model trichothecene T-2 toxin and satratoxin G regarding the possible role of DNA damage and associated downstream pathways.

## MATERIALS AND METHODS

**Reagents.** RPMI 1640 culture medium and fetal bovine serum (FBS) were obtained from Gibco BRL (Paisley, Scotland). All other chemicals used were purchased from commercial sources at highest purity available. Antibody toward phospho-(p)ATM (s1981, #AF 1655) was purchased from R & D Systems, whereas phosphospecific antibody toward PKR (pTyr 451, #AT-7137) was purchased from MBL International Corporation. Antibodies toward apoptosis inducing factor (AIF) (#4642), cleaved poly(ADP-ribose)polymerase (PARP) (#9544),  $\beta$ -actin (#4967), endonuclease G (endoG) (#4969), Chk2 (Thr 68, #2661), Chk1 (Ser 345, #2341),  $\gamma$ H2AX (Ser 139, #2577), direct-conjugated  $\gamma$ H2AX-Fluor Alexa 488 antibody, and phospho-p38 (thr180/Tyr 182, #9211) were all purchased from Cell Signaling. Low melting point agarose (LMPA) and normal melting point agarose (NMPA) were from Invitrogen. Formamidopyrimidine DNA glycosylase (fpg) was kindly provided by Andrew Collins (University of Oslo, Norway). ATM small interfering RNA (siRNA) (sc-29761) was purchased from Santa Cruz Biotechnology. The broad-spectrum caspase inhibitor Z-VAD-FMK was from Alexis Biochemicals, pure T-2 toxin and the ATM inhibitor KU 55933 were from Sigma-Aldrich, whereas the p38 inhibitor SB 202190 was purchased from Calbiochem. Satratoxin G was purified from *S. chartarum* cultures as previously described (Islam *et al.*, 2009).

**Cell cultures.** The human THP-1 monocyte cell line was cultured in RPMI 1640 medium with 10% (vol/vol) fetal calf serum, to which 100 µg/ml gentamicin and 4-(2-hydroxyethyl)-1-piperazineethanesulfonic acid (HEPES) were added. Media were replaced every 2–3 days. Studies were performed at densities of  $1 \times 10^6$  cells/ml. All cell preparations were performed at room temperature using aseptic techniques in a laminar flow hood.

**Mold spore preparation.** Mold cultures were obtained from Biocentrum-DTU (Denmark Technical University). These included *S. chartarum* IBT 9631 (satratoxin producer), *S. chartarum* IBT 9634 (atranone producer), and *A. versicolor* IBT 3781 (sterigmatocystin producer). The strains were densely spread on 90-mm malt extract agar plates (Samson *et al.*, 2004) and incubated upside down in perforated plastic bags at  $25 \pm 1^\circ\text{C}$  in the dark for 14 days before harvesting of the conidia. One milliliter sterile tap water was added to each plate, and the spores were carefully scraped off by means of a sterile L-shaped spreader. Spores and water from one single agar plate were then transferred to one sterile 2-ml Eppendorf tube. After immediate autoclaving of the Eppendorf tubes in glass jars at  $121^\circ\text{C}$  for 15 min, they were cooled and stored at  $4 \pm 1^\circ\text{C}$  until use. The heat treatment killed the conidia, whereas the toxins are considered heat resistant.

Satratoxin G in *S. chartarum* IBT 9631 spore preparation was confirmed by ELISA (Chung *et al.*, 2003). Spores were microfuged and the aqueous phase diluted (1:5 and 1:25) and analyzed by ELISA. The latter was readable in our standard curve. The IBT 9631 strain contained satratoxin G at a concentration of  $\sim 3 \times 10^{-8}$  µg/spore. Satratoxin G was not detected in the other two spore preparations.

**Assessment of cell death.** THP-1 cells were exposed to various concentrations of the *S. chartarum* spores (0.1, 0.5, or  $1.0 \times 10^7$  spores/million cells), *A. versicolor* spores (0.5, 1.0, 4.0, or  $8.0 \times 1.0 \times 10^7$  spores/million cells), or T-2 toxin (4 µM) for either 3 or 6 h. The T-2 concentration was chosen based on reported concentrations used with Jurkat cells (Shifrin and Anderson, 1999) and alveolar macrophages (Gerberick and Sorenson, 1983) and because similar responses were observed for IBT 9631 spores and this concentration of T-2 toxin. Plasma membrane damage and changes in nuclear morphology associated with necrosis and apoptosis of the THP-1 cells were determined after staining cells ( $\sim 1.0 \times 10^6$  cells) with propidium iodide (PI; 10 µg/ml) and Hoechst 33342 (5 µg/ml) (Sigma Chemical Company, MO) for 30 min. Smears made from THP-1 cells suspended in FBS were air dried quickly. Cell morphology was evaluated using a Nikon Eclipse E400 fluorescence microscope. Cells with distinct condensed nuclei, segregated nuclei, and apoptotic bodies were counted as apoptotic and determined as a fraction of the total number of cells. Non-apoptotic cells, excluding PI, were categorized as viable cells. PI-stained cells with a round morphology and homogeneously stained nucleus were termed PI positive.

**Immunocytochemistry.** To investigate presence and localization of proteins associated with cell death and DNA damage after 3-h exposure to spores or T-2 toxin, cells were stained for AIF, endoG, cleaved PARP, γH2AX, and phosphorylated ataxia telangiectasia mutated. Briefly, after exposure, cells were washed in PBS and fixed in methanol for 3 min before incubation for 20 h with rabbit anti-AIF, endoG, PARP, or γH2AX (all in working dilution 1:500) at room temperature. After washing and incubation with an anti-rabbit fluorescein-isothiocyanate-conjugated antibody for 3 h, the preparations were mounted and visualized using a Nikon Eclipse E400 microscope and a SPOT diagnostic instruments digital camera. As controls, the secondary antibody was omitted.

**Western blotting.** THP-1 cells were seeded and exposed on 33-mm<sup>2</sup> culture dishes at a density of  $1.0 \times 10^6$  cells/cm<sup>2</sup>. After exposure, the cells were harvested in ice-cold PBS containing phenylmethanesulfonyl (1 mM). Isolated total protein (12.5–25 µg) was electrophoresed (Laemmli, 1970), blotted onto nitrocellulose filters, and analyzed using specific antibodies (Towbin *et al.*, 1979). To confirm equal levels of protein in each well, Ponceau staining and β-actin were used as loading controls. Filters were blocked with 3% Bovine Serum Albumin (BSA) in tris buffered saline (TBS)-Tween (0.1% [vol/vol] Tween 20) and then incubated with primary antibodies diluted in TBS-Tween

containing 1% (wt/vol) BSA. Working dilutions of 1:4000 (p-Chk2, γH2AX, and p-Chk1) and 1:5000 (β-actin) were found to be appropriate for immunoblotting. Immunoreactive protein was detected using a chemiluminescence system according to the manufacturer's instructions (Super-Signal West Dura chemoluminescence system, Thermo Scientific, IL) after incubation with horseradish peroxidase-conjugated secondary antibody. Optical quantification of the protein bands was performed using the KODAK 1D Image Analysis Software.

**Transfection by electroporation.** Transfection was performed by electroporation with Nucleofector from Amaxa Biosystems (Cologne, Germany) using optimized program and solutions recommended by the manufacturer (Cell Line Nucleofector Kit V [VCA-1003]). Cells were grown in T175 bottles, trypsinized, collected by centrifugation ( $250 \times g$ , 10 min), and resuspended in nucleofector solution at two cell suspensions of  $2 \times 10^5$  and  $1 \times 10^6$  cells per 100 µl and 3 µg siRNA were added to cells and samples were transferred into certified cuvettes (Amaxa Biosystems) and transfected by using program U-01. Cells were then seeded on 6-well plates in prewarmed medium, supplemented with 10% fetal calf serum. The next day (24 h posttransfection), transfected cells were exposed to the different spore types or T-2 toxin for 3 h. After exposure, the cells were harvested for Western blotting or stained with Hoechst/PI for evaluation of cell death.

**Flow cytometry.** Exposed cells and controls were washed once in PBS, fixed in 1% (wt/vol) paraformaldehyde (PFA) in PBS 15 min on ice, and postfixed in 90% (vol/vol) ice-cold methanol for at least 2 days at  $-20^\circ\text{C}$ . The cells were then washed two times in 5% (wt/vol) BSA in PBS and incubated with primary antibody, p-Chk2 1:25, cleaved caspase 3 1:200, or the direct-conjugated γH2AX-Fluor Alexa 488 antibody 1:10 in 5% (wt/vol) BSA and 0.2% (vol/vol) Triton X-100 in PBS overnight at  $4^\circ\text{C}$ . The cells stained with primary antibody were then rinsed twice in 5% BSA in PBS and incubated with secondary antibody conjugated to Fluor Alexa 488 1:500 (Invitrogen) for 2 h at room temperature in the dark. The cells were then analyzed with an LSRII Flow Cytometer (BD Biosciences), and 10,000 cells were measured. The number of T-2 toxin-exposed cells expressing p-Chk2, cleaved caspases 3, or γH2AX-Fluor Alexa was compared with the number of cells expressing these proteins in the unexposed control group.

**Deoxynucleotidyl transferase-mediated fluorescein-dUTP nick end-labeling.** We used an In Situ Cell Death Detection Kit, TMR red (Roche Diagnostics, GmbH) to label the apoptotic cells and analyzed them by flow cytometry. Cells were washed by PBS, fixed in 1% (wt/vol) PFA on ice for 15 min, and postfixed in 90% (vol/vol) ice-cold methanol for at least two days at  $-20^\circ\text{C}$ . The cells were then washed once in PBS and incubated with deoxynucleotidyl transferase-mediated fluorescein-dUTP nick end-labeling (TUNEL) reaction mixture for 60 min at  $37^\circ\text{C}$  in a dark and humidified atmosphere. Subsequently, the cells were washed twice in PBS, transferred to tubes, and directly analyzed by flow cytometry. The cells were excited with a blue Argon laser (15 mW) at 488 nm, and the fluorescence was recorded and analyzed.

**Comet assay.** The comet assay was performed at alkaline pH. Following exposure, the cells were washed twice in cold PBS and 10,000 cells in 10 µl PBS were resuspended in 75 µl 1% LMPA at  $37^\circ\text{C}$  and applied onto glass slides (precoated with 1% NMPA and dried) and covered with cover slips. Two equal gels were made on each slide. The slides were placed at  $4^\circ\text{C}$  for 10 min to allow the gel to set. The cover slips were then removed and the slides were immersed in prechilled lysis buffer (2.5M NaCl, 0.1M EDTA, 10mM Tris-HCl, pH 10, and 1% Triton X-100) and incubated at  $4^\circ\text{C}$  overnight. After lysis, the slides were washed three times in washing buffer (40mM HEPES, 0.1M KCl, 0.5mM EDTA, and 0.2 mg/ml BSA pH 8) at  $4^\circ\text{C}$  for 5 min. One of the two gels at each slide was treated with 50 µl fpg diluted in washing buffer (1:3000) and covered with a cover slip made of parafilm. The other gel on the slide was treated with washing buffer only. The slides were then placed horizontally in a humidity chamber at  $37^\circ\text{C}$  for 30 min. After enzyme treatment, the slides were immersed in a cold alkali solution (0.3M NaOH and 1mM EDTA, pH > 13) for 30 min following electrophoresis in a prechilled alkali solution (0.3M NaOH

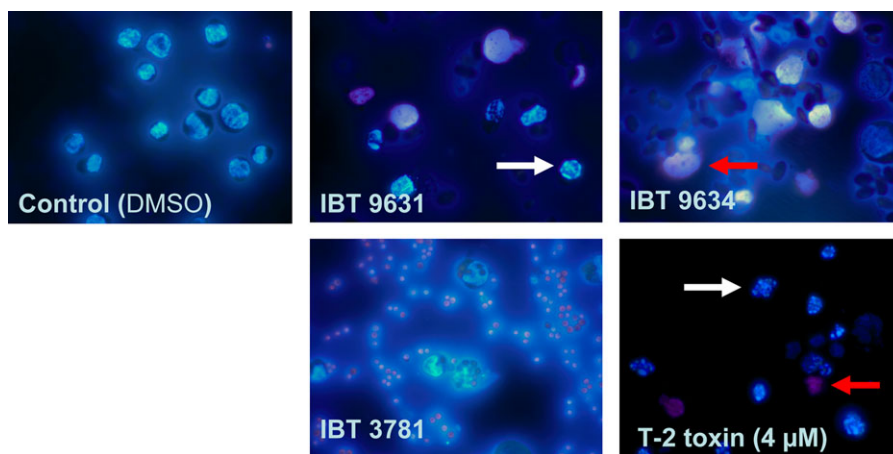


**FIG. 1.** Microscopic view of control (DMSO treated) and spores- or T-2 toxin-treated THP-1 cells. Cells were exposed to *S. chartarum* IBT 9631, IBT 9634 (both  $0.5 \times 10^7$  spores/million cells), *A. versicolor* IBT 3781 ( $4.0 \times 10^7$  spores/million cells), or T-2 toxin ( $4\mu\text{M}$ ) for 6 h, stained with Hoechst 33342 and PI, and analyzed by fluorescence microscopy. White arrows indicate apoptotic cells and red arrows indicate necrotic cells.

and 1mM EDTA, pH > 13) on 1 V/cm for 30 min and air dried on the bench. The slides were stained with SYBR green (1:10 000) for 10 min and images were visualized under a fluorescence microscope (Olympus BX51; Olympus Europe, Hamburg, Germany) and acquired with an Olympus DP70 camera. A minimum of 100 comets on each slide were analyzed using the TriTek CometScore Freeware (www.tritekcorp.com). The differences in tail intensity between fpg-treated cells (total DNA damage) and untreated cells (basic DNA damage) were considered as 8-oxodGuo (oxidative DNA damage).

**Detection of ROS.** ROS measurements were performed by means of a dichlorofluorescein assay (Wang and Joseph, 1999). Stock solution of dichlorofluorescein diacetate (DCFH-DA) was dissolved in dimethyl sulfoxide (DMSO) to a final concentration of 100mM. The cells were plated on 6-well plastic dishes and incubated at  $37^\circ\text{C}$  in a humidified atmosphere of 5%  $\text{CO}_2$  in air for 30 min with DCFH-DA added to a final concentration of  $5\mu\text{M}$ . Excess DCFH-DA was removed after 30 min and the cells washed and incubated with buffer containing the specified concentrations of pure satratoxin G, T-2 toxin, or spores. After 30-min exposure, the content of the wells were transferred to vials and the fluorescence of the cells from each well measured by flow cytometry (Cell Lab Quanta SC MPL; Beckman Coulter). The excitation filter was set at 488 nm, and the emission filter was set at 525 nm. The fluorescence from each well was captured, digitized, and stored.

**Statistics.** The data were analyzed using Student's *t*-test ( $p < 0.05$ ), Kruskal-Wallis one-way ANOVA ( $p < 0.05$ ), or ANOVA with all pairwise multiple comparison procedures (Holm-Sidak method) ( $p < 0.001$ ) to evaluate the difference between groups.

## RESULTS

### Cell Death in THP-1 Cells after Exposure to Different Spore Isolates and T-2 toxin

The human THP-1 macrophage cell line was exposed to heat-treated spores from *S. chartarum* IBT 9631, *S. chartarum* IBT 9634, *A. versicolor* IBT 3781, or the model trichothecene T-2 toxin for 6 h. As judged by microscopy, exposure to satratoxin-producing *S. chartarum* IBT 9631 and T-2 resulted in apoptosis, whereas exposure to atranone-producing *S. chartarum* IBT 9634 and sterigmatocystin-producing *A. versicolor* IBT 3781 caused mostly

necrosis (Fig. 1). Concentration experiments (6 h) showed that assessed by their overall cell death inducing potential, IBT 9631 was most potent, followed by IBT 9634 and IBT 3781 (Fig. 2a).

Based on the data from the concentration experiments, time course experiments were conducted on cells exposed to  $0.5 \times 10^7$  spores/million cells (IBT 9631 and 9634),  $4.0 \times 10^7$  spores/million cells (IBT 3781), or to  $4\mu\text{M}$  T-2 toxin for 3 and 6 h. The results are shown in Figure 2b. IBT 9631 and T-2 toxin caused the highest levels of apoptosis at both exposure times, and the increase was significantly higher after 6 h compared to 3 h. Thus, the apoptotic process induced by IBT 9631 spores and T-2 toxin was rapid and completed within 3–6 h.

### Induction of Apoptosis by *S. chartarum* IBT 9631 Spores and T-2 toxin

To further characterize and verify the induction of apoptosis, cells were assessed for the activation of various biochemical markers. Activation of caspase 3 is often found to be central in the apoptotic process and known to mediate cleavage of PARP and activate DNA endonucleases resulting in DNA fragmentation that can be detected by the TUNEL assay. Immunocytochemistry using specific antibody toward cleaved PARP showed that exposure of THP-1 cells to either the satratoxin G-containing IBT 9631 spores or the T-2-toxin led to an increased number of cells with a higher fluorescence after both 3 and 6 h (Fig. 3a). In contrast, less changes were seen in the spores from the other *Stachybotrys* strain, IBT 9634. Flow cytometry revealed that exposure to T-2 toxin led to DNA fragmentation as measured by the TUNEL assay as exposure resulted in a time-dependent right shift in fluorescence. A similar right shift was seen using an antibody toward the active form of caspase 3 (Figs. 3b and 3c). These results support our suggestion that the apoptotic cells characterized

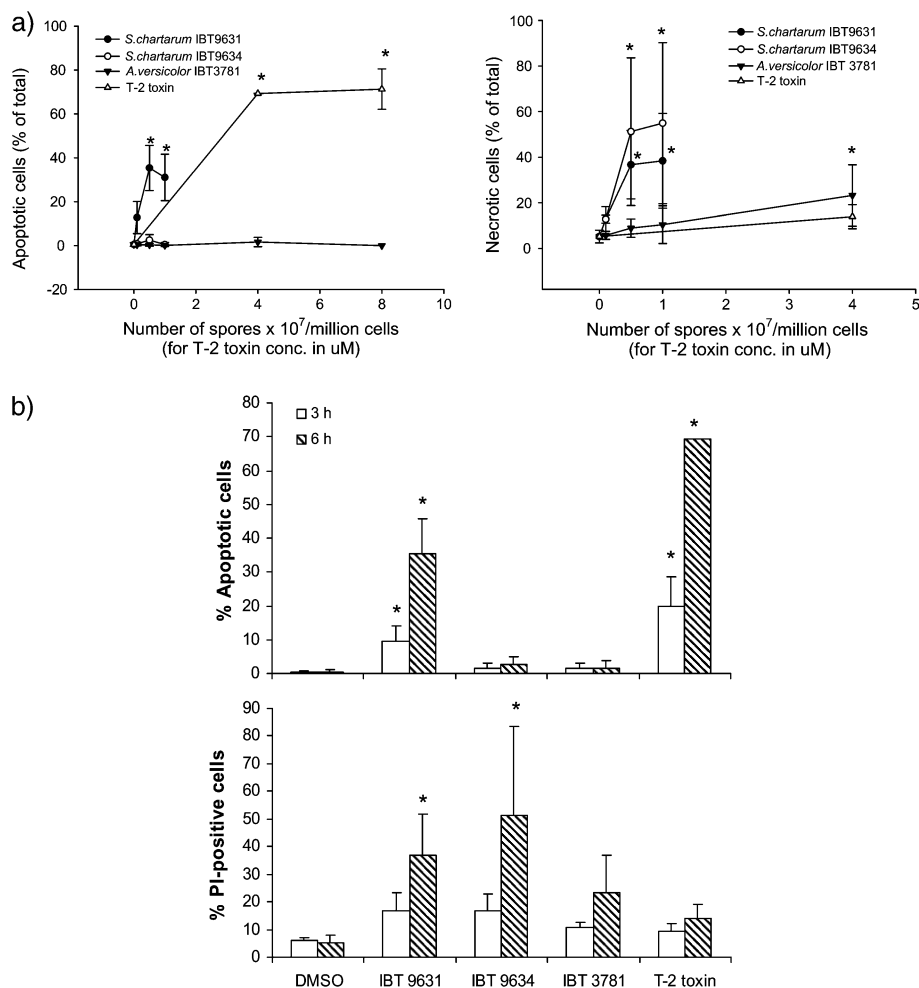


**FIG. 2.** Cell death induced by spores or T-2 toxin treatment. (a) Concentration-dependent changes in apoptosis and necrosis in THP-1 cells after exposure to spores or T-2 toxin for 6 h. Cells were stained with Hoechst 33342 and PI and analyzed by fluorescence microscopy. Results are shown as percent apoptotic or necrotic cells of total cell number. Values represent mean  $\pm$  SD of at least  $n = 3$  experiments. \*Statistical difference from control ( $p < 0.05$ ). (b) Increased apoptosis and necrosis in THP-1 cells after exposure to spores or T-2 toxin for 3 and 6 h. The concentrations of spores were  $0.5 \times 10^7$  spores/million cells (*S. chartarum* IBT 9631 and IBT 9634) or  $4.0 \times 10^7$  spores/million cells (*A. versicolor* IBT 3781), whereas the toxin concentration was  $4 \mu$ M. Cells were stained with Hoechst 33342 and PI and analyzed by fluorescence microscopy. Results are shown as percent apoptotic or necrotic cells of total cell number. Values represent mean  $\pm$  SD of at least  $n = 3$  experiments. \*Statistical difference from control ( $p < 0.05$ ).

by microscopic examination after Hoechst staining are rather classic apoptotic cells.

#### Effects of Exposure to Different Spore Isolates and T-2-toxin on Phosphorylation of PKR

Based on data indicating involvement of PKR activation in apoptosis after exposure to some mycotoxins, we wanted to explore if this was the case in the response to our spore isolates and T-2 toxin. Thus, we examined the activation of PKR by Western blotting after 3-h exposure. The results showed reduced activation of PKR after exposure to IBT 9631 spores or T-2 toxin (Fig. 4). Furthermore, no phosphorylation of PKR following exposure to spores or toxin was detected at the early time points investigated (10- and 30-min exposure) (data not shown).

#### Oxidative DNA Damage in THP-1 Cells Exposed to Different Spore Isolates and T-2 toxin

When comet assay was used to detect DNA damage forming single-stranded DNA breaks (SSB) (Collins *et al.*, 2008), none of the exposures resulted in any increased DNA damage measured by an increased tail moment. After the addition of fpg, an enzyme that converts 8-oxo-7,8-dihydro-2'-guanosine (8-oxodGuo) to SSB, an increase in tail moment could be seen after all spore exposures (Fig. 5a), although this increase was significant only after IBT 9631 and IBT 9634 exposure. Compared to its respective control with DMSO, no significant increase in tail moment was seen after exposure to T-2 toxin.

ROS induce oxidative damage of DNA, including strand breaks and base and nucleotide modifications. Oxidative modification induces a repair response, characterized by

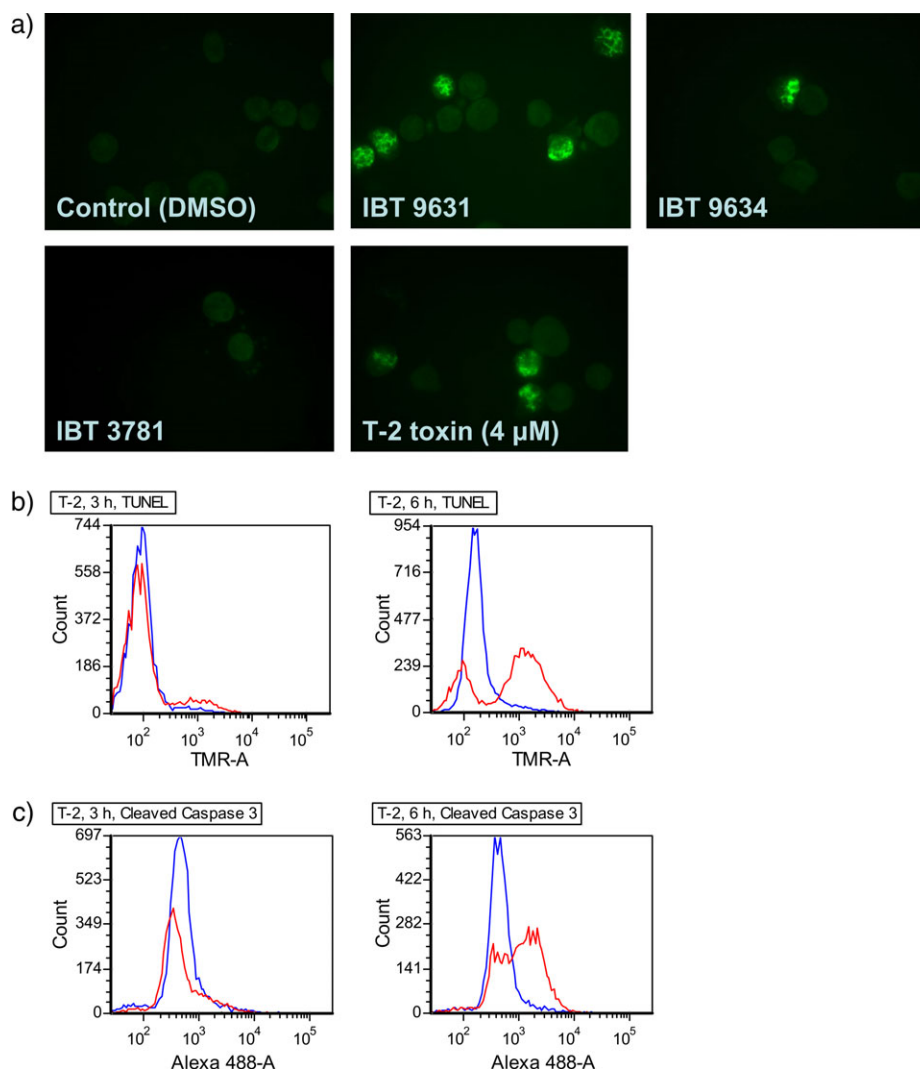


**FIG. 3.** Apoptosis induced by spores or T-2 toxin treatment. (a) Apoptosis induced by *S. chartarum* IBT 9631 measured by immunofluorescence. The concentrations of spores were  $0.5 \times 10^7$  spores/million cells (*S. chartarum* IBT 9631 and IBT 9634) or  $4.0 \times 10^7$  spores/million cells (*A. versicolor* IBT 3781), whereas the toxin concentration was  $4 \mu\text{M}$ . Pictures of cells stained with antibodies against the apoptotic marker cleaved PARP after exposure for 3 h. (b) Apoptosis induced by T-2 toxin ( $4 \mu\text{M}$ ) measured by TUNEL assay after 3 and 6 h exposure. Blue lines represent control cells (DMSO treated) and red lines represent toxin-exposed cells. Increase in TMR intensity indicates increased levels of free 3' OH ends in DNA, resulting from apoptotic DNA strand breaks. (c) Apoptosis induced by T-2 toxin ( $4 \mu\text{M}$ ) measured by flow cytometry analysis of cells stained with antibodies against the apoptotic marker cleaved caspase 3 after 3 and 6 h exposure. Blue lines represent control cells (DMSO treated) and red lines represent toxin-exposed cells. Increase in Alexa 488 intensity indicates increased levels of cleaved caspase 3 in the cells.

excision of modified bases and nucleotides. Double-stranded DNA breaks activate DNA repair enzymes, including ATM and ATR. Using the fluorochrome DCFH-DA and flow cytometry, we found that all spore types seemed able to increase ROS formation (Fig. 5b). The highest increase (and only one significantly higher than control) was seen after exposure to the IBT 9631 spores. No increased ROS formation was detected after exposure to T-2 toxin alone (data not shown).

#### Effect of Ascorbic Acid (Vitamin C) on Cell Death

To elucidate the effect of ROS formation on cell death, we pretreated the cells with vitamin C ( $0.3 \text{ mM}$ ) for 30 min

and assessed its impact on apoptotic and necrotic cell death after exposure to spores or T-2 toxin for 6 h. As judged by microscopy, the apoptosis induced by the satratoxin-producing *S. chartarum* IBT 9631 was significantly reduced in the cells treated with vitamin C (Fig. 6). No effect of vitamin C was detected on cell death in controls or on necrosis.

#### Effects of Exposure to Different Spore Isolates and T-2 Toxin on ATM Phosphorylation

To further explore the involvement of a possible primary DNA damage, we examined the activation of enzymes

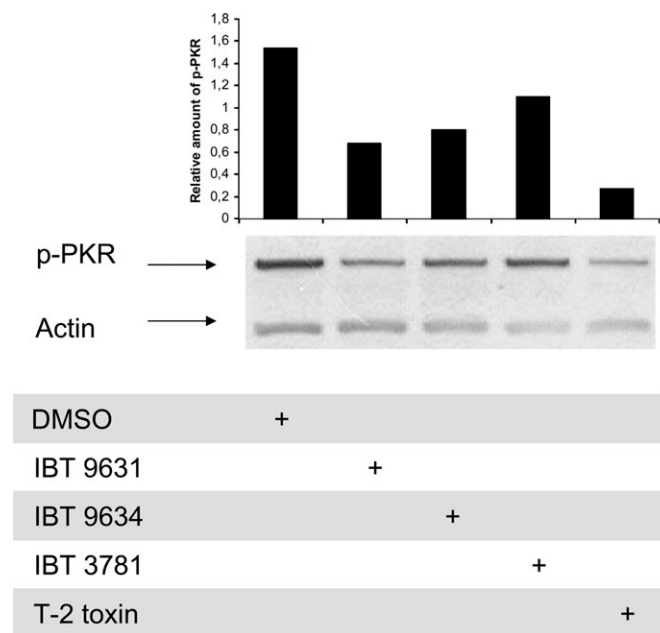


**FIG. 4.** Reduced PKR activation in THP-1 cells after exposure to either spores or T-2 toxin. THP-1 cells were exposed to  $0.5 \times 10^7$  spores/million cells (*S. chartarum* IBT 9631 and IBT 9634),  $4.0 \times 10^7$  spores/million cells (*A. versicolor* IBT 3781), or 4  $\mu$ M T-2 toxin for 3 h. PKR expression was analyzed by Western blotting. To determine the total amount of protein, blots were stripped and reprobbed with anti-actin polyclonal antibody. The blots were quantified and the relationship between phosphorylated PKR protein and total protein is shown as horizontal bars on top of the figure.

involved in DNA damage responses after exposure to spores or T-2 toxin. First, we looked at the phosphorylation of ATM, which is suggested to be triggered by DSBs and/or larger chromatin changes. At all investigated exposure times (2 h, shown and 3 h, not shown), all three spore types, as well as T-2 toxin, were able to cause nuclear phosphorylation of ATM, whereas no nuclear ATM phosphorylation was observed in unexposed cells (Fig. 7). No marked differences between the various exposures were seen (data not shown). Furthermore, no changes in phosphorylation of ATR, another enzyme known to be activated by DNA damage, were observed.

#### Effects of Exposure to Different Spore Isolates and T-2 Toxin on Chk1 and Chk2 Phosphorylation

Chk1 and Chk2 are kinases that are involved in cell cycle checkpoint signaling and considered to be triggered by the activation of ATR and ATM, respectively. None of the exposures increased the phosphorylation of Chk1 (data not shown), but exposure of THP-1 cells to either IBT 9631 spores or T-2-toxin increased the phosphorylation of Chk2 (Fig. 8a). In contrast, no changes were seen after exposure to IBT 9634 or IBT 3781 spores. The phosphorylation of Chk2 protein in THP-1 cells after T-2 toxin exposure was confirmed with flow cytometry (Fig. 8b).

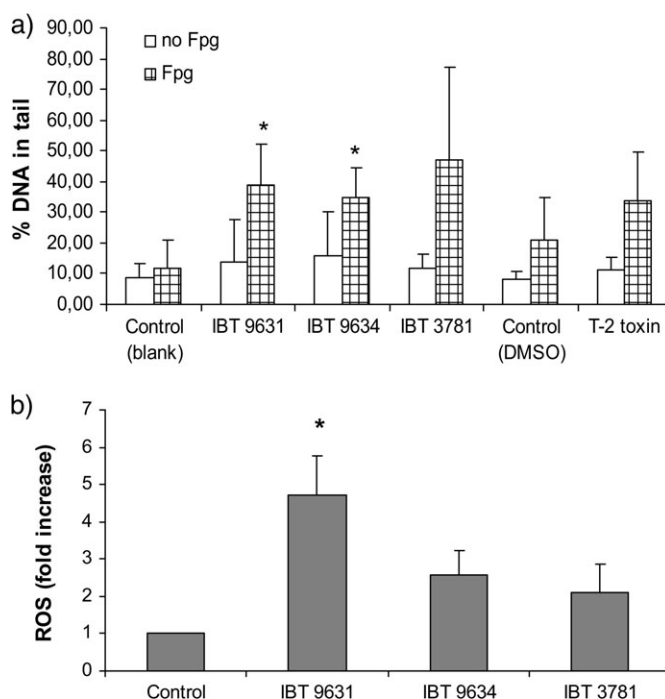


**FIG. 5.** DNA damage and ROS formation after exposure to spores or T-2 toxin. (a) Single-cell gel electrophoresis analysis (comet assay) of cells exposed to  $0.5 \times 10^7$  spores/million cells (*S. chartarum* IBT 9631 and IBT 9634),  $4.0 \times 10^7$  spores/million cells (*A. versicolor* IBT 3781), or 4  $\mu$ M T-2 toxin for 3 h. The data show DNA damage measured as percent DNA in tail of  $\pm$  fpg enzyme-treated cells. Values represent mean  $\pm$  SD of  $n = 4$  experiments. \*Statistical difference from respective control ( $p < 0.05$ ). (b) THP-1 cells were exposed to  $0.5 \times 10^7$  spores/million cells (*S. chartarum* IBT 9631 and IBT 9634) or  $4.0 \times 10^7$  spores/million cells (*A. versicolor* IBT 3781) for 30 min. ROS formation was analyzed by flow cytometry. Results are shown as fold increase over control. Values represent mean  $\pm$  SD of  $n = 3$  experiments. \*Statistical difference from control ( $p < 0.05$ ).

#### Effects of the ATM Inhibitor KU 55933 and ATM siRNA on Spore- and T-2 Toxin-Induced Chk2 Phosphorylation

To ascertain if the increased phosphorylation of Chk2 was mediated through ATM kinase, we pretreated the cells with KU 55933, a chemical inhibitor of this enzyme. Western blots of cell lysates revealed that KU 55933 reduced the increased levels of phosphorylated Chk2 seen after IBT 9631 and T-2 treatments (Fig. 8c).

To gain further insight into the possible upstream role of ATM in phosphorylation of Chk2, we transfected the cells with ATM siRNA before exposure. Western blotting revealed that the transfection reduced the level of phosphorylated Chk2 associated with IBT 9631 or T-2 toxin exposure compared with what was seen with nontransfected cells (Fig. 8d).

#### Effects of Exposure to Different Spore Isolates and T-2 Toxin on $\gamma$ H2AX Expression

DSBs initiate phosphorylation of H2AX. Thus, the detection of its phosphorylated form, termed  $\gamma$ H2AX, is a widely used tool to study the formation and repair of DSBs. Exposure of

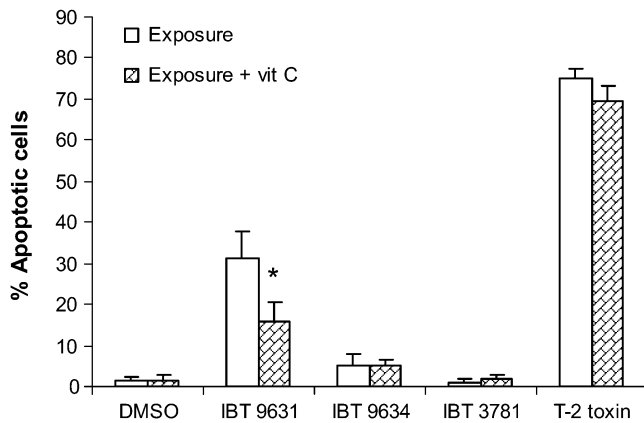


**FIG. 6.** Effects of preincubation with vitamin C on spore- or T-2 toxin-induced apoptosis. THP-1 cells were preincubated for 30 min with vitamin C before exposure to spores or T-2 toxin for 6 h. The concentrations of spores were  $0.5 \times 10^7$  spores/million cells (*S. chartarum* IBT 9631 and IBT 9634) or  $4.0 \times 10^7$  spores/million cells (*A. versicolor* IBT 3781), whereas the toxin concentration was  $4\mu\text{M}$ . Cells were stained with Hoechst 33342 and analyzed by fluorescence microscopy. Results are shown as percent apoptotic cells of total cell number. Values represent mean  $\pm$  SD of  $n = 3$  parallels in one experiment. \*Significant reduction in apoptosis in vitamin C-treated IBT 9631 group compared to IBT 9631 treatment only ( $p < 0.05$ ).

THP-1 cells to either IBT 9631 spores or T-2 toxin, but not IBT 9634 or IBT 3781 spores, caused increased expression of  $\gamma\text{H2AX}$  (Fig. 9a) which was confirmed using flow cytometry (Fig. 9b).

#### Effects of the ATM Inhibitor KU 55933 and ATM siRNA on Spore- and T-2 Toxin-Induced $\gamma\text{H2AX}$ Expression

H2AX is also directly phosphorylated by ATM. To explore any possible role of ATM in the activation of H2AX, we pretreated cells with KU 55933 and exposed them to IBT 9631

spores. The immunocytochemical staining of  $\gamma\text{H2AX}$  positive cells showed a reduced number of positive cells when KU 55933 was added compared to the identical exposure group not pretreated with inhibitor (Fig. 9c). Transfection with ATM siRNA prior to exposure reduced the levels of  $\gamma\text{H2AX}$  associated with IBT 9631 or T-2 toxin exposure compared with what was seen with nontransfected cells (Fig. 9d).

#### Rapid Effects of Exposure to *S. chartarum* IBT 9631 on $\gamma\text{H2AX}$ and Phospho-p38 Expression

Western blotting revealed that IBT 9631 rapidly activated H2AX, as shown at 15-min exposure time (Fig. 10a). A similar pattern was also seen after 30-min (Fig. 10b) and 60-min exposure (data not shown).

Recent findings have suggested that p38 is able to activate H2AX. To elucidate a role for p38 in our model, we ran the same Western blot (15-min exposure) with an antibody against phosphorylated p38. The results showed that the rapid phosphorylation of H2AX occurred concurrently with p38 activation (Fig. 10a). Furthermore, if the cells were pretreated with the p38 inhibitor SB 202190, *S. chartarum* IBT 9631 did not induce any significant phosphorylation of H2AX when compared to its respective control, suggesting a link between p38 activation and activation of H2AX (Fig. 10b).

#### Z-VAD-FMK Treatment and Effect on $\gamma\text{H2AX}$ after Exposure to either *S. chartarum* IBT 9631 or T-2 Toxin for 3 h

To elucidate the effect of caspase activation on H2AX activation, we treated the cells with the broad-spectrum caspase inhibitor Z-VAD-FMK ( $20\mu\text{M}$ ) and assessed its impact on H2AX activation. Cells were treated with the inhibitor 30 min before exposure. The results indicated no substantial reduction in H2AX activation (Fig. 11).

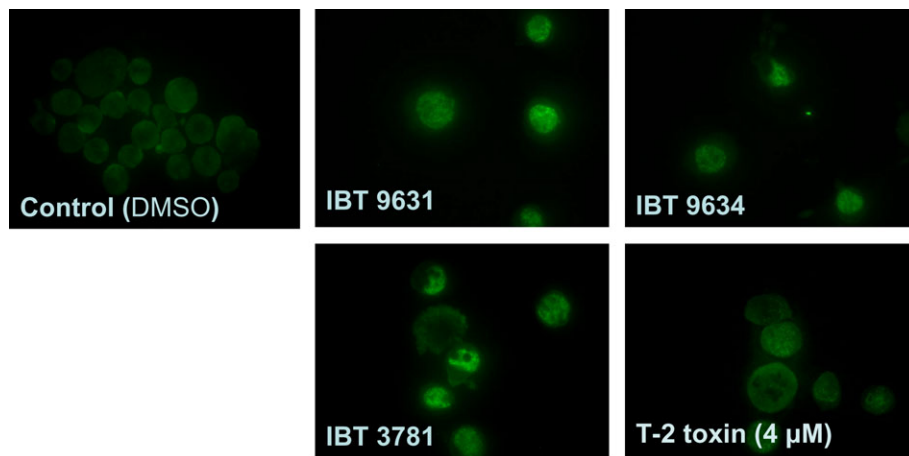


**FIG. 7.** Phosphorylation of ATM induced in THP-1 cells after exposure to spores or T-2 toxin. Activation of ATM was analyzed by immunocytochemistry. Cells were stained with a specific antibody against the phosphorylated form of ATM. Cells were exposed to  $0.5 \times 10^7$  spores/million cells (*S. chartarum* IBT 9631 and IBT 9634),  $4 \times 10^7$  spores/million cells (*A. versicolor* IBT 3781), or  $4\mu\text{M}$  T-2 for 2 h.

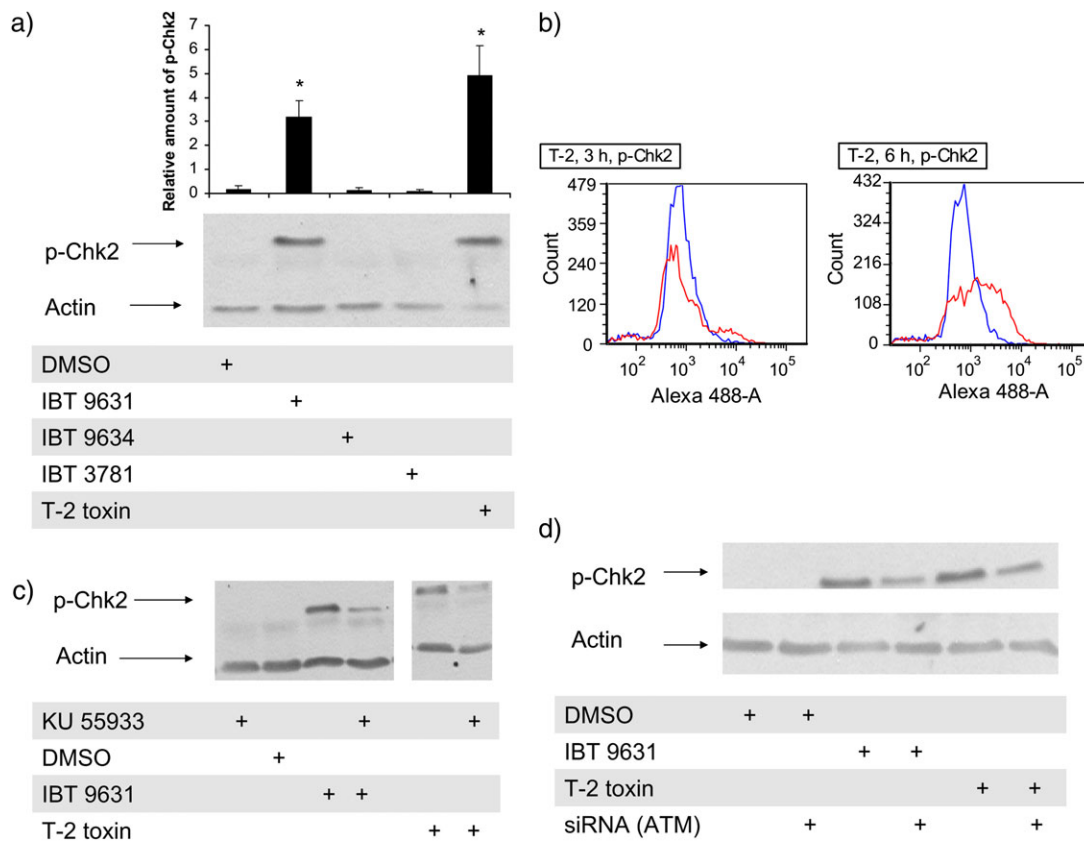


**FIG. 8.** Phosphorylation of Chk2 induced in THP-1 cells after exposure to spores or T-2 toxin. (a) Cells were exposed to  $0.5 \times 10^7$  spores/million cells (*S. chartarum* IBT 9631 and IBT 9634),  $4.0 \times 10^7$  spores/million cells (*A. versicolor* IBT 3781), or 4 μM T-2 for 3 h. Phosphorylation of Chk2 was analyzed by Western blotting. Blots were washed and re probed with an anti-actin polyclonal antibody. The blots were quantified and the relationship between the level of Chk2 and actin is shown as horizontal bars on top of the figure. Values represent mean  $\pm$  SD of  $n = 3$  experiments. \*Statistical difference from control ( $p < 0.05$ ). One representative blot is shown. (b) Phosphorylation of Chk2 analyzed by flow cytometry after exposure of THP-1 cells to 4 μM T-2 toxin for 3 and 6 h. Blue lines represent control cells (DMSO treated) and red lines represent toxin-exposed cells. Increase in Alexa 488 intensity indicates presence of phosphorylated Chk2 in the cells. (c) Effects of the ATM inhibitor KU 55933 on spore- or toxin-induced phosphorylation of Chk2. Cells were preincubated with or without inhibitor (5 μM) for 1 h, followed by incubation with  $0.5 \times 10^7$  spores/million cells (*S. chartarum* IBT 9631) or 4 μM T-2 toxin for 3 h. Effects on phosphorylation of Chk2 were analyzed by Western blotting. (d) Effects of siRNA against ATM on spore- or toxin-induced phosphorylation of Chk2. Cells were transfected by electroporation with ATM siRNA before exposure to  $0.5 \times 10^7$  spores/million cells (*S. chartarum* IBT 9631) or 4 μM T-2 toxin for 3 h. Effects on phosphorylation of Chk2 were analyzed by Western blotting.

#### Effects of Exposure to Different Spore Isolates and T-2 Toxin on AIF

AIF and endoG are often found to be translocated from the mitochondria to the nucleus where they have been suggested to participate in larger DNA fragmentation resulting in partial nuclear chromatin condensation. To examine if the activation of Chk2 and H2AX was related to a translocation of these enzymes, the cells were stained for AIF and endoG and examined after 3-h exposure. No significant changes in the staining pattern for AIF or endoG were found for any of the exposure groups (data not shown), suggesting that they were not the cause of the observed DNA damage signaling.

#### Effects of Satratoxin G

To further verify that satratoxin might be involved in the main effects observed after exposure to IBT 9631 spores, we

exposed the cells to satratoxin G for 3 or 6 h and at different concentrations and assayed the apoptotic response by fluorescence microscopy. The results showed a modest apoptotic response at 3 h, whereas robust apoptosis was detected after 6 h at 10 ng/ml (Fig. 12). This effect increased with higher concentrations (data not shown).

Next, we determined whether satratoxin G was able to give a similar rapid DNA damage response as that observed after IBT 9631 spore exposures. The results demonstrated that satratoxin G at a concentration of 10 ng/ml activated H2AX as well as p38 within 15 min (Fig. 13). This activation of H2AX was also observed after 30-min, 1-h, and 3-h exposure times (data not shown). Finally, we investigated whether exposure to satratoxin G was able to induce ROS formation. However, no significant increased ROS formation was detected by flow cytometry at the time point tested (1 h, data not shown).

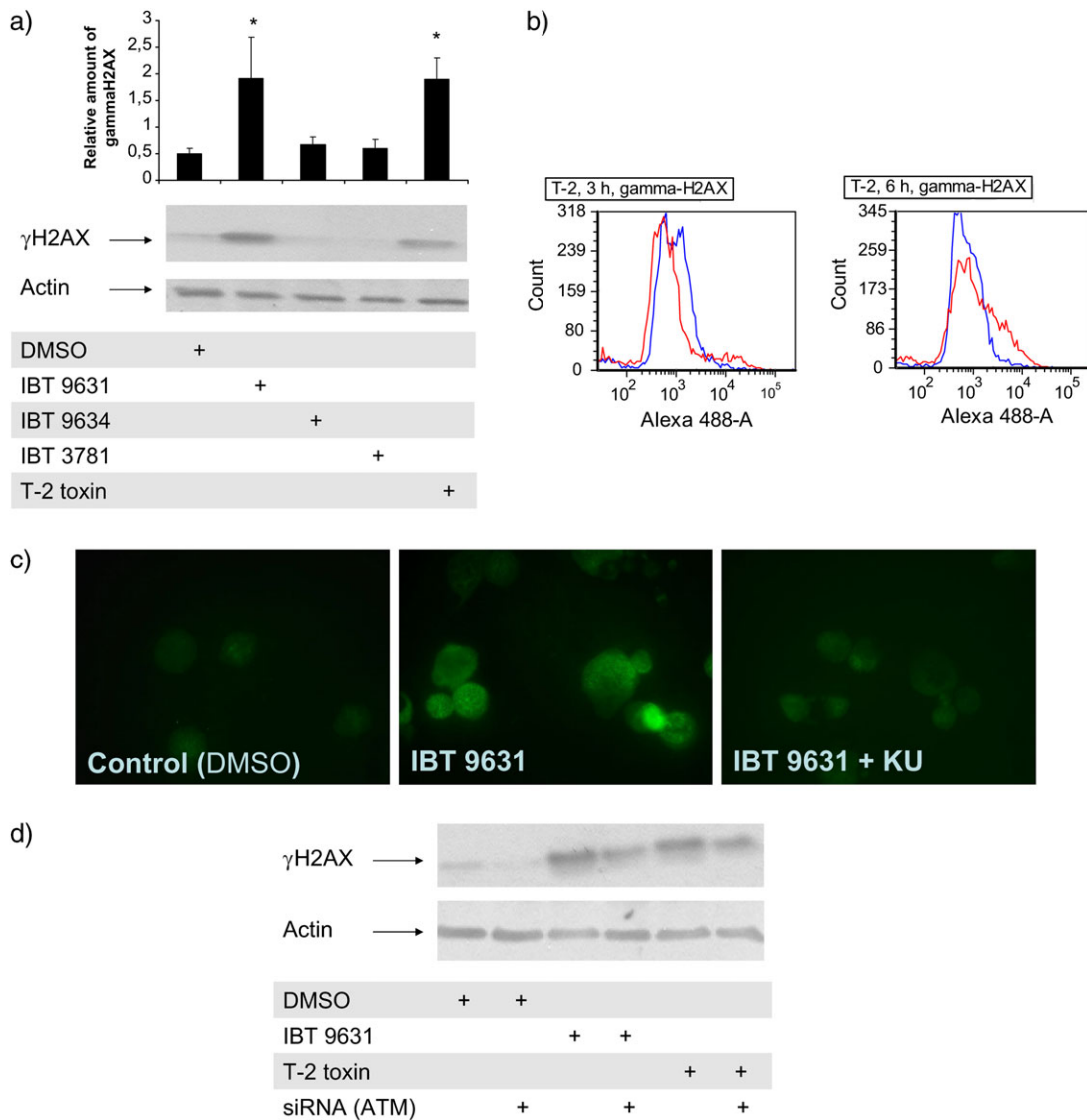


**FIG. 9.** Phosphorylation of H2AX induced in THP-1 cells after exposure to spores or T-2 toxin. (a) Phosphorylation of H2AX analyzed by Western blotting after exposure to  $0.5 \times 10^7$  spores/million cells (*S. chartarum* IBT 9631 and IBT 9634),  $4.0 \times 10^7$  spores/million cells (*A. versicolor* IBT 3781), or  $4 \mu\text{M}$  T-2 toxin for 3 h. The blots were split in two and the part where  $\gamma\text{H2AX}$  was expected to localize based on molecular weight was probed with antibody against  $\gamma\text{H2AX}$ , whereas the other part was probed with anti-actin polyclonal antibody. The blots were quantified and the relationship between the levels of  $\gamma\text{H2AX}$  and actin is shown as horizontal bars on top of the figure. Values represent mean  $\pm$  SD of  $n = 3$  experiments. \*Statistical difference from control ( $p < 0.05$ ). One representative blot is shown. (b) Levels of  $\gamma\text{H2AX}$  analyzed by flow cytometry after exposure of THP-1 cells to  $4 \mu\text{M}$  T-2 toxin for 3 and 6 h. Blue lines represent control cells (DMSO treated) and red lines represents toxin-exposed cells. Increase in Alexa 488 intensity indicates presence of  $\gamma\text{H2AX}$  in the cells. (c) Effects of the ATM inhibitor KU 55933 on spore-induced phosphorylation of H2AX. Cells were preincubated with or without inhibitor ( $5 \mu\text{M}$ ) for 1 h, followed by incubation with  $0.5 \times 10^7$  spores/million cells (*S. chartarum* IBT 9631) for 3 h. Effects on presence of  $\gamma\text{H2AX}$  were analyzed by immunofluorescent staining of the cells. (d) Effects of siRNA against ATM on spore- or toxin-induced phosphorylation of H2AX. Cells were transfected by electroporation with ATM siRNA before exposure to  $0.5 \times 10^7$  spores/million cells (*S. chartarum* IBT 9631) or  $4 \mu\text{M}$  T-2 toxin for 3 h. Effects on levels of  $\gamma\text{H2AX}$  were analyzed by Western blotting.

## DISCUSSION

*Stachybotrys chartarum* are known to produce several macrocyclic trichothecenes, with satratoxins regarded as the most important. Also, other mycotoxins may be produced but with less characterized biological activity. There is considerable variation among isolates of *S. chartarum* in the production of mycotoxins and other metabolites, and two chemotypes of

the fungus, the atranone and the macrocyclic trichothecene producers, have been proposed. The present study demonstrates that some of the adverse effects of *S. chartarum* spores in mononuclear phagocytes are associated with the presence of trichothecene mycotoxins. Based on the early DNA damage response after exposure to *S. chartarum* IBT 9631 spores or the two trichothecenes employed here, DNA damage is likely to be

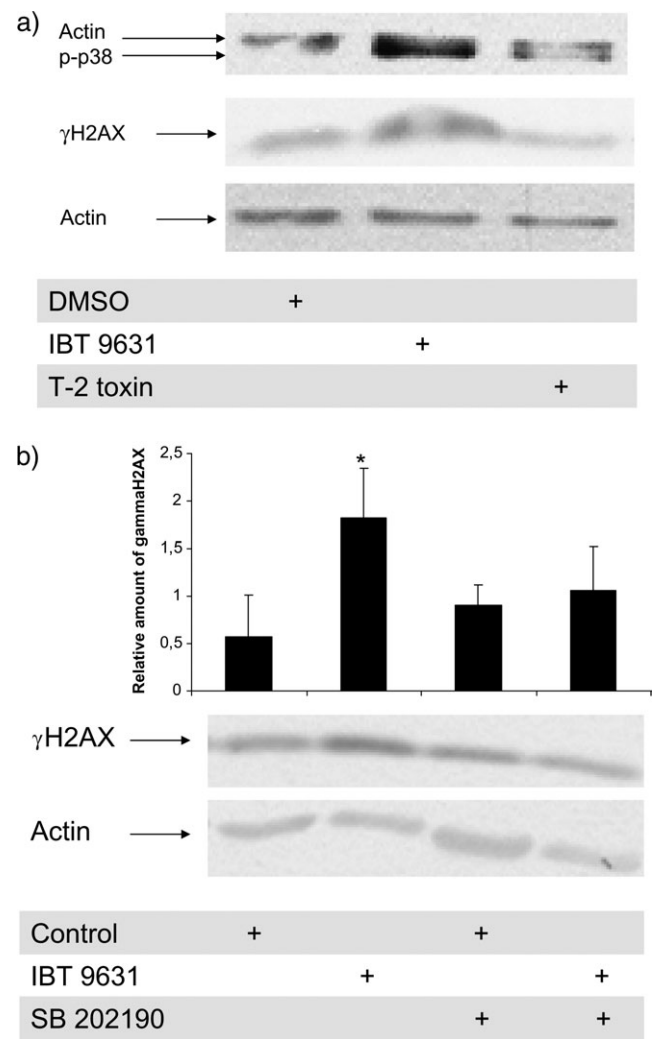


**FIG. 10.** Rapid effects of exposure to *S. chartarum* IBT 9631 on  $\gamma$ H2AX and phospho-p38 expression in THP-1 cells. (a) The activation of H2AX and p38 after 15-min exposure to *S. chartarum* IBT 9631 ( $0.5 \times 10^7$  spores/million cells) was analyzed by Western blotting. The blot was split in two and the part where  $\gamma$ H2AX was expected to localize was probed with antibody against  $\gamma$ H2AX, whereas the other part was probed with an anti-actin polyclonal antibody. Next, the part of the blot where actin localized was washed and reprobbed with an antibody against phospho-p38. One representative blot is shown. (b) Effect of the p38 inhibitor SB 202190 on *S. chartarum* IBT 9631-induced activation of H2AX. Cells were preincubated with or without inhibitor (10 $\mu$ M) for 30 min, followed by incubation with  $0.5 \times 10^7$  spores/million cells (*S. chartarum* IBT 9631) for 30 min. The blots were quantified and the relationship between  $\gamma$ H2AX and actin is shown as horizontal bars on top of the figure. \*A significant increase in H2AX activation compared to its respective control. Values represent mean  $\pm$  SD of  $n = 3$  experiments. One representative blot is shown.

one of the triggering mechanisms involved in the toxic response. In addition, activation of the MAPK p38 appears to be another important early event in the apoptotic process.

The IBT 9631 isolate employed here was found to produce the macrocyclic trichothecene satratoxin G at a concentration of  $\sim 3 \times 10^{-8}$   $\mu$ g satratoxin G/spore. This is in accordance with concentrations previously reported by others (Kelman *et al.*,

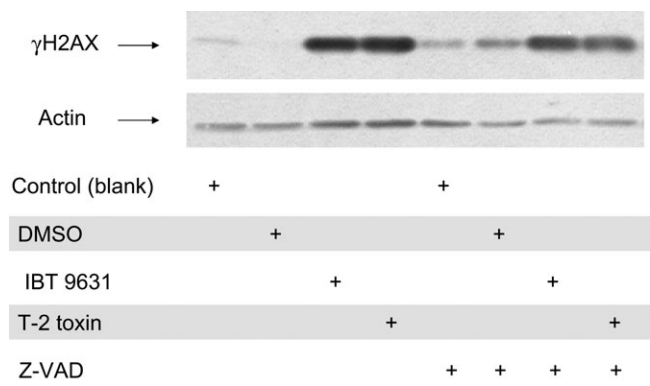


**FIG. 11.** Lack of effect of caspase inhibitor on  $\gamma$ H2AX expression. The effect of the broad-spectrum caspase inhibitor Z-VAD-FMK on  $\gamma$ H2AX expression was analyzed by Western blotting. Cells were preincubated with or without inhibitor (20 $\mu$ M) for 30 min, followed by exposure to either *S. chartarum* IBT 9631 ( $0.5 \times 10^7$  spores/million cells) or T-2 toxin (4 $\mu$ M) for 3 h.

2004). IBT 9634 preparations were likely to contain atranone based on data from the supplier (no quantification given). When the THP-1 cells were exposed to the spores from *S. chartarum*, IBT 9631 and IBT 9634, having the same size and morphology but having different chemotype mycotoxins, we observed different types of cell death. Specifically, the satratoxin G-producing IBT 9631 strain induced both apoptosis and necrosis, whereas the atranone-producing IBT 9634 strain induced necrosis only. These findings are in line with previous findings in other cell lines (RAW 264.7 murine macrophages, PC-12 murine neuronal cells, and human leukemia HL-60 cells), showing that satratoxin G induces apoptosis (Bae *et al.*, 2009; Nagase *et al.*, 2002). Consistent with these findings, the model trichothecene T-2 toxin also rapidly induced high levels of apoptosis in THP-1 cells, which is in accordance with other observations (Bouaziz *et al.*, 2009). Based on an overall evaluation of the different potency and response pattern obtained by the various exposures, as well as previous studies (Pestka *et al.*, 2008), our findings support the contention that toxic effects of *S. chartarum* spores result in part from the type and amount of associated mycotoxins. The most important seems to be the highly toxic satratoxins, which also were detected in the present study. This suggestion is further supported by our additional experiments showing that pure satratoxin G induced similar responses as observed with IBT 9631. However, this does not exclude the possibility that other mycotoxins or spore components as well as the spores as particles may be involved in our observed responses. Interestingly, it has been reported that mold/spores including *S. chartarum* sequester different proteinases, which ordinarily may have an impact on exposed cells (Yike *et al.*, 2007). This could be important in an *in vivo* situation, but is not likely to occur in our system, as heat treatment of the spores reduces the activity of these proteinases.

Apoptosis following exposure to the spores with mycotoxin or T-2 toxin was rapid and based on morphological

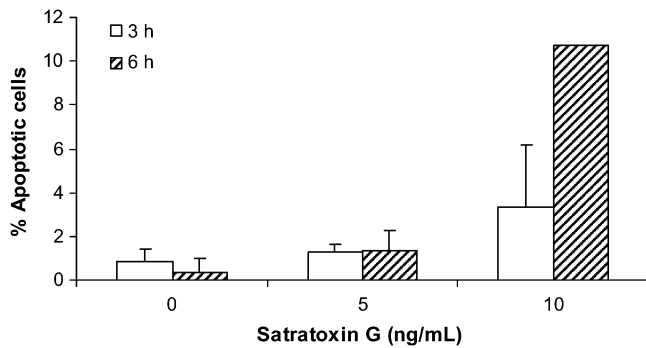


**FIG. 12.** Apoptosis induced by satratoxin G treatment. Increased apoptosis in THP-1 cells after exposure to two different concentrations of satratoxin G for 3 and 6 h. Cells were stained with Hoechst 33342 and analyzed by fluorescence microscopy. Results are shown as percent apoptotic cells of total cell number. Values represent mean  $\pm$  SD of  $n = 3$  experiments (except for 10 ng/ml, where  $n = 2$ ).

examination, completed by 3–6 h. A similar fast apoptotic process after exposure to mycotoxins has also previously been reported (Fujii *et al.*, 2003; Holme *et al.*, 2003; Nagase *et al.*, 2002). By comparison, no increase in the amount of apoptotic cells is observed after exposure to chemicals such as polycyclic aromatic hydrocarbons before 18–24 h (Holme *et al.*, 2007; Solhaug *et al.*, 2004) or in some experimental systems not before 48–72 h (Huc *et al.*, 2006). Nevertheless, apoptosis induced by satratoxin-producing IBT 9631 and T-2 toxin was conventional based on activation of caspase 3, cleavage of PARP, DNA fragmentation and condensation, and fragmentation of nuclei.

Various suggestions to how satratoxin G triggers apoptosis have been reported, indicating that mechanisms might vary by cell type. The apoptotic process in HL-60 human leukemia cells seems to involve activation of caspase 8 and triggering of the mitochondrial pathway involving cytosolic accumulation of cytochrome c and activation of caspase 9 (Nagase *et al.*, 2002).

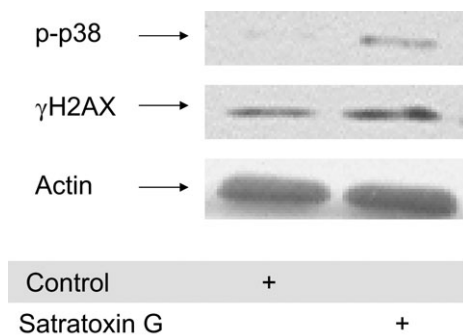


**FIG. 13.** Rapid effects of exposure to satratoxin G on phospho-p38 and  $\gamma$ H2AX expression in THP-1 cells. The activation of p38 and H2AX after 15-min exposure to satratoxin G (10 ng/ml) was analyzed by Western blotting. The blot was split in two and the part where phospho-p38 was expected to localize was probed with antibody against phospho-p38, whereas the other part was probed with an antibody against  $\gamma$ H2AX. Next, the part of the blot where phospho-p38 localized was washed and reprobed with anti-actin polyclonal antibody.

Similarly, T-2 toxin has also been reported to induce apoptosis through a caspase-dependent pathway involving the mitochondria, both in HL-60 cells (Holme *et al.*, 2003) and in human hepatoma HepG2 cells (Nagase *et al.*, 2001; Bouaziz *et al.*, 2008). However, other possibilities exist. Recently, satratoxin G was found to induce apoptosis in murine PC-12 neuronal cells via a caspase-independent pathway apparently involving AIF (Islam *et al.*, 2008). This process was mediated by PKR and possibly triggered by interaction with the ribosomes. In line with this, previous studies have reported that another trichothecene, DON, also activates PKR (Zhou *et al.*, 2003). Furthermore, the use of specific inhibitors and siRNA suggested that PKR plays a central role in DON-induced gene expression. Specifically, PKR appears to mediate MAPK activation and apoptosis following ribotoxic stress initiated by the trichothecene. In contrast, we did not find PKR to have a major role in the IBT 9631- and T-2 toxin-mediated toxic response in the THP-1 cell line. Exposure to both IBT 9631 and T-2 toxin rather reduced the phosphorylation of PKR at the time points examined (3 h shown, as well as 10 and 30 min, data not shown). Furthermore, the addition of its inhibitor (tested at several concentrations) did not reduce the satratoxin G-containing spore- and T-2 toxin-induced effects, including phosphorylation of H2AX, and rather increased their apoptotic effects (data not shown).

A possible explanation for the above findings could be that the PKR pathway described after DON exposure is reported to involve p53, which is not expressed in THP-1 cells (Sugimoto *et al.*, 1992). In accordance with our findings, however, a recent study reported that PKR seems to increase the protein expression level and phosphorylation of Bcl-2 and plays an antiapoptotic role in human hepatocellular carcinoma cells (HepG2) (Yang and Chan, 2009). Such a mechanism where inhibition of PKR decreases Bcl-2 phosphorylation and induces apoptosis would be in line with our findings. Furthermore, in this model, c-Jun N-terminal kinase (JNK) was suggested to be involved. This is also in agreement with our findings that inhibition of JNK (data not shown) reduced IBT 9631-induced apoptosis at 3-h exposure. Interestingly, Islam *et al.* (2008) reported that an inhibition of PKR also reduced satratoxin G-induced expression of AIF and its translocation to the nucleus. Thus, a lack of p53 function and an inhibition of PKR may explain the lack of AIF translocation in the THP-1 cells after exposure to IBT 9631 in the present study.

A number of studies have suggested that mycotoxins may induce DNA damage. Previous studies have indicated that some mycotoxins may interact directly with DNA. Interestingly, macrocyclic trichothecenes have epoxides in their chemical structure, similar to the DNA-binding epoxide in the bioactivated aflatoxin B<sub>1</sub> (Choy, 1993), indicating their potential as genotoxic agents. Several studies have reported that mycotoxins may cause oxidative DNA damage (Iwahashi *et al.*, 2007; Wang and Groopman, 1999). Furthermore, methanol extracts of a trichothecene-producing strain of

*S. chartarum* were found to increase the amount of single-strand DNA breaks as measured by the alkaline comet assay (Wang and Yadav, 2006). In the present study, we found that the *Stachybotrys* spores gave a significant effect in the comet assay after addition of fpg, giving support for the presence of induced oxidative DNA damage. An increase, although not significant, was also observed with the *Aspergillus* spores. The somewhat variable responses observed may be due to handling and/or aging of the spores as the trichothecene-epoxides may bind to SH-groups on proteins. However, we show that vitamin C significantly reduced the IBT 9631-induced apoptosis, supporting that oxidative damage was inflicted at least by this spore type. By flow cytometry, we were also able to show that all spore types caused increased ROS formation, with IBT 9631 being clearly the most potent. This is in agreement with the overall ATM activation that we observe after spore exposure. Although no ROS formation was observed after exposure to the pure toxins in this study, there are studies that have reported this (Chaudhari *et al.*, 2009; Wang and Yadav, 2006).

Interestingly, previous studies have shown that satratoxin G may increase the number of micronuclei, which are often related to increased levels of DSBs. The possibility that various mycotoxins may induce DSBs is to some extent supported by our results showing that all spore and T-2 toxin exposures induced some ATM activation and that the satratoxin G-producing IBT 9631 spores and T-2 toxin caused a specific activation of the checkpoint proteins Chk2 and H2AX. Additional experiments demonstrated a similar activation of H2AX after exposure to pure satratoxin G, supporting that this toxin is an important contributor to the IBT 9631 spore response. Several studies have identified ATM kinase as a major sensor of DSBs (Efeyan and Serrano, 2007; Ljungman, 2005). Similarly, Chk2 and H2AX have also commonly been found to be activated by DSBs. However, it should be noted that  $\gamma$ H2AX also can be induced by DNA lesions other than DSBs, i.e., intermediates in repair of other DNA damage as well as DSBs formed during DNA replication (Chadwick and Lane, 2005; Marti *et al.*, 2006; Smart *et al.*, 2008). When activation of ATM and H2AX is induced by formation of DSB, the activated ATM is localized in individual discrete foci as assessed by immunocytochemistry (Rogakou *et al.*, 1999). In contrast, ATM and H2AX activation triggered by other DNA lesions or chromatin alterations induces a diffusely scattered staining pattern throughout the nucleoplasm (Bakkenist and Kastan, 2003; Kitagawa and Kastan, 2005; Tanaka *et al.*, 2007b). Our immunocytochemical results rather show the presence of such diffuse staining, leaving the possibility that the activation of DNA damage proteins we see is caused by DNA damage other than DSBs. Overall, the results regarding the DNA damage response pattern induced suggest that the satratoxin G-producing IBT 9631 spores induce different type of DNA damage compared to the atranone-producing IBT 9634. Still it seems as the spores induce ROS formation

and oxidative DNA damage by acting as particles and hence independent of the associated mycotoxins.

It is notable that the *S. chartarum* IBT 9634 and *A. versicolor* IBT 3781 strains did not induce Chk2/H2AX phosphorylation and mostly resulted in necrosis. In contrast, exposure to IBT 9631 and T-2 resulted in Chk2/H2AX phosphorylation and apoptotic cell death, suggesting that Chk2/H2AX activation could be an important mechanism for initiation of apoptosis. Also, a reduced phosphorylation of both Chk2 and H2AX following treatments with inhibitors and siRNA toward ATM indicates that ATM was involved in the activation of these enzymes but that the activation of ATM *per se* was not sufficient for further activation of downstream DNA damage response proteins. In this context, it is worth noting that phosphorylation of ATM on serine 1981 does not necessarily indicate that downstream targets will be phosphorylated in an ATM-dependent manner (Kurz and Lees-Miller, 2004).

To understand whether H2AX phosphorylation is triggered by a primary DNA damage or is merely a reflection of DNA fragmentation during apoptosis, it is critical to distinguish these two outcomes (Tanaka *et al.*, 2007a). The H2AX activation was observed at a very early time point after exposure to IBT 9631 (15 and 30 min), whereas activation of caspase 3 was observed much later (3–6 h). Interestingly, the same rapid activation of H2AX was observed after exposure to pure satratoxin G. This supports the notion that spores with satratoxin G as well as pure satratoxin G induced a DNA damage response directly and not as a secondary response to stalled DNA repair or replication, far less as a secondary response to DNA cleavage occurring during apoptosis. This notion is also supported by the observed lack of Chk1 and ATR activation, the latter being regarded as a main sensor of stalled replication forks and DNA adduct formation. It is also interesting to note that a recent report shows that the mycotoxin alternariol may act as a topoisomerase toxin, thereby resulting in DSBs. This could be an interesting mechanistic possibility also for satratoxin G and T-2 toxin that should be explored, although the present  $\gamma$ H2AX response may seem too fast to make this a likely explanation (Fehr *et al.*, 2009).

Our results suggest that the downstream activation of Chk2 and H2AX by ATM may require the activity of additional kinases. Previous results have indicated that a DON-induced activation of p53 was depending on an early phosphorylation of p38 (Zhou *et al.*, 2005a), suggesting that p38 could be needed for a direct phosphorylation of p53 or possibly act on upstream activators of p53. Such an upstream signal could include Chk2. With regard to H2AX, it has been reported by Lu *et al.* (2006) that JNK can phosphorylate H2AX and suggested a role for this event in response to UVA radiation. However, in the present study, we did not see an increased early activation of JNK, suggesting no role for JNK in the rapid activation of H2AX observed after exposure to IBT 9631. A more plausible candidate is therefore the p38 MAPK pathway, which is reported to be activated after various

responses to environmental stress, including DSBs (Zarubin and Han, 2005). Interestingly, a recent study reported that serum starvation-induced H2AX phosphorylation was dependent on p38 (Lu *et al.*, 2008), and a novel signaling pathway (p38/H2AX) to regulate apoptosis was proposed. Accordingly, we found rapid and concomitant activation of both p38 and H2AX short time after exposure to IBT 9631.

A similar activation of p38 was seen after exposure to satratoxin G and somewhat weaker after exposure to T-2 toxin at the same early time point (15 min). Furthermore, an inhibition of p38 before exposure to IBT 9631 reduced the activation of H2AX, suggesting that p38 partly was involved in the phosphorylation of H2AX. Trichothecene-induced apoptosis has previously been reported to involve activation of p38, as well as JNK and extracellular signal-regulated kinase (Wang and Yadav, 2006; Yang *et al.*, 2000; Zhou *et al.*, 2005b). Other studies have demonstrated that inhibition of p38 MAPK activity with the p38-specific inhibitor SB203580 had no effect on satratoxin G-induced apoptosis, whereas it moderately inhibited apoptosis induced by the trichothecene vomitoxin (Yang *et al.*, 2000). Thus, the role of p38 in trichothecene-induced apoptosis seems to vary somewhat depending on the mycotoxin and model used.

A pivotal question is what activates the early p38 phosphorylation that we observe. One possibility could be that satratoxin G-induced DSBs or a similar event could activate caspase 2. Interestingly, it has been shown that caspase 2 in complex with TRAF2 and RIP1 is capable of activating p38 MAPK through the caspase recruitment domain of caspase 2, independently of its proteolytic activity (Lamkanfi *et al.*, 2005). Taken that this caspase is involved, its independence of proteolytic activity may explain why we did not find the caspase inhibitor to have a profound effect on H2AX activation. However, the lack of effect of the inhibitor does not exclude the possibility of the presence of a two-stage activation of H2AX, a rapid one involving activation by p38 and a later one induced by secondary DNA fragmentation occurring during apoptosis.

In conclusion, while all spores induced ROS formation and oxidative DNA damage by acting as particles, it seems that the observed differences in cell death patterns after exposure to different spore isolates are likely to be primarily due to the types of mycotoxins that the spores produce. Our results further show that spores containing satratoxin G as well as satratoxin G and T-2 toxin without spores may induce a DNA damage response that involves activation of the ATM/H2AX/Chk2 pathway. The process, which seems to be regulated by the p38 MAPK, is suggested to be important in the caspase-dependent apoptosis triggered by these agents.

## FUNDING

Research Council of Norway (153875/310 to R.B.); U.S. Public Health Service Grant (ES03553 to J.J.P.).

## REFERENCES

- Bae, H. K., Shinozuka, J., Islam, Z., and Pestka, J. J. (2009). Satratoxin G interaction with 40 S and 60 S ribosomal subunits precedes apoptosis in the macrophage. *Toxicol. Appl. Pharmacol.* **237**, 137–145.
- Bakkenist, C. J., and Kastan, M. B. (2003). DNA damage activates ATM through intermolecular autophosphorylation and dimer dissociation. *Nature* **421**, 499–506.
- Bouaziz, C., Martel, C., Sharaf el dein, O., Abid-Essefi, S., Brenner, C., Lemaire, C., and Bacha, H. (2009). Fusarial toxin-induced toxicity in cultured cells and in isolated mitochondria involves PTPC-dependent activation of the mitochondrial pathway of apoptosis. *Toxicol. Sci.* **110**, 363–375.
- Bouaziz, C., Sharaf, E. D., El Golli, E., Abid-Essefi, S., Brenner, C., Lemaire, C., and Bacha, H. (2008). Different apoptotic pathways induced by zearalenone, T-2 toxin and ochratoxin A in human hepatoma cells. *Toxicology* **254**, 19–28.
- Burma, S., Chen, B., Murphy, M., Kurimassa, A., and Chen, D. J. (2001). ATM phosphorylates histone H2AX in response to DBS. *J. Biol. Chem.* **276**, 42462–42467.
- Chadwick, B. P., and Lane, T. F. (2005). BRCA1 associates with the inactive X chromosome in late Sphase, coupled with transient H2AX phosphorylation. *Chromosoma* **114**, 432–439.
- Chaudhari, M., Jayaraj, R., Bhaskar, A. S., and Lakshmana Rao, P. V. (2009). Oxidative stress induction by T-2 toxin causes DNA damage and triggers apoptosis via caspase pathway in human cervical cancer cells. *Toxicology* **262**, 153–161; Epub 2009 June 12.
- Choy, W. N. (1993). A review of the dose–response induction of DNA adducts by aflatoxin B1 and its implications to quantitative cancer-risk assessment. *Mutat. Res.* **296**, 181–198.
- Chung, Y. J., Jarvis, B. B., Tak, H., and Pestka, J. J. (2003). Immunochemical assay for satratoxin G and other macrocyclic trichothecenes associated with indoor air contamination by *Stachybotrys chartarum*. *Toxicol. Mech. Meth.* **13**, 247–252.
- Cole, R., and Cox, R. (1981). In *Handbook of Toxic Fungal Metabolites*. Academic Press, New York.
- Collins, A. R., Oscoz, A. A., Brunborg, G., Gaivão, I., Giovannelli, L., Kruszewski, M., Smith, C. C., and Stetina, R. (2008). The comet assay: topical issues. *Mutagenesis* **23**, 143–151.
- Cundliffe, E., and Davies, J. E. (1977). Inhibition of initiation, elongation, and termination of eukaryotic protein synthesis by trichothecene fungal toxins. *Antimicrob. Agents Chemother.* **11**, 491–499.
- Efeyan, A., and Serrano, M. (2007). p53: guardian of the genome and policeman of the oncogenes. *Cell Cycle* **6**, 1006–1010.
- Engelhart, S., Looock, A., Skutlarek, D., Sagunski, H., Lommel, A., Färber, H., and Exner, M. (2002). Occurrence of toxigenic *Aspergillus versicolor* isolates and sterigmatocystin in carpet dust from damp indoor environments. *Appl. Environ. Microbiol.* **68**, 3886–3890.
- Etzel, R. A. (2002). Mycotoxins. *JAMA* **287**, 425–427.
- Fehr, M., Pahlke, G., Fritz1, J., Christensen, M. O., Boege, F., Altemöller, M., Podlech, J., and Marko, D. (2009). Alternariol acts as a topoisomerase poison, preferentially affecting the Ila isoform. *Mol. Nutr. Food Res.* **53**, 441–451.
- Fujii, J., Matsui, T., Heatherly, D. P., Schlegel, K. H., Lobo, P. I., Yutsudo, T., Ciralo, G. M., Morris, R. M., and Obrig, T. (2003). Rapid apoptosis induced by Shiga toxin in HeLa cells. *Infect. Immun.* **71**, 2724–2735.
- Gerberick, G. F., and Sorenson, W. G. (1983). Toxicity of T-2 toxin, a Fusarium mycotoxin, to alveolar macrophages in vitro. *Environ. Res.* **32**, 269–285.
- González-Flecha, B. (2004). Oxidant mechanisms in response to ambient air particles. *Mol. Aspects Med.* **25**, 169–182.

- Gopalakrishnan, S., Liu, X., and Patel, D. J. (1992). Solution structure of the covalent sterigmatocystin-DNA adduct. *Biochemistry* **31**, 10790–10801.
- Green, B. J., Schmechel, D., Sercombe, J. K., and Tovey, E. R. (2005). Enumeration and detection of aerosolized *Aspergillus fumigatus* and *Penicillium chrysogenum* conidia and hyphae using a novel double immunostaining technique. *J. Immunol. Methods* **307**, 127–134.
- Hardin, B. D., Kelman, B. J., and Saxon, A. (2003). Adverse human health effects associated with molds in the indoor environment. *J. Occup. Environ. Med.* **45**, 470–478.
- Holme, J. A., Gorria, M., Arlt, V. M., Ovrebø, S., Solhaug, A., Tekpli, X., Landvik, N. E., Huc, L., Fardel, O., and Lagadic-Gossman, D. (2007). Different mechanisms involved in apoptosis following exposure to benzo[a]pyrene in F258 and Hepa1c17 cells. *Chem. Biol. Interact.* **167**, 41–55.
- Holme, J. A., Morrison, E., Samuelsen, J. T., Wiger, R., Låg, M., Schwarze, P. E., Bernhoft, A., and Refsnes, M. (2003). Mechanisms involved in the induction of apoptosis by T-2 and HT-2 toxins in HL-60 human promyelocytic leukemia cells. *Cell Biol. Toxicol.* **19**, 53–68.
- Huc, L., Rissel, M., Solhaug, A., Tekpli, X., Gorria, M., Torriglia, A., Holme, J. A., Dimanche-Boitrel, M. T., and Lagadic-Gossman, D. (2006). Multiple apoptotic pathways induced by p53-dependent acidification in benzo[a]pyrene-exposed hepatic F258 cells. *J. Cell. Physiol.* **208**, 527–537.
- Islam, Z., Hegg, C. C., Bae, H. K., and Pestka, J. J. (2008). Satratoxin G-induced apoptosis in PC-12 neuronal cells is mediated by PKR and caspase independent. *Toxicol. Sci.* **105**, 42–52.
- Islam, Z., Shinozuka, J., Harkema, J. R., and Pestka, J. J. (2009). Purification and comparative neurotoxicity of the trichothecenes satratoxin G and roridin L2 from stachybotrys chartarum. *J. Toxicol. Environ. Health A* **72**, 1242–1251.
- Iwahashi, H., Kitagawa, E., Suzuki, Y., Ueda, Y., Ishizawa, Y., Nobumasa, H., Kuboki, Y., Hosoda, H., and Iwahashi, Y. (2007). Evaluation of toxicity of the mycotoxin citrinin using yeast ORF DNA microarray and Oligo DNA microarray. *BMC Genomics* **8**, 95.
- Kelman, B. J., Robbins, C. A., Swenson, L. J., and Hardin, B. D. (2004). Risk from inhaled mycotoxins in indoor office and residential environments. *Int. J. Toxicol.* **23**, 3–10.
- Kitagawa, R., and Kastan, M. B. (2005). The ATM-dependent DNA damage signaling pathway. *Cold Spring Harb. Symp. Quant. Biol.* **70**, 99–109.
- Kurz, E. U., and Lees-Miller, S. P. (2004). DNA damage-induced activation of ATM and ATM-dependent signaling pathways. *DNA Repair* **3**, 889–900.
- Laemmli, U. K. (1970). Cleavage of structural proteins during the assembly of the head of bacteriophage T4. *Nature* **227**, 680–685.
- Lamkanfi, M., D'hondt, K., Walle, L. V., van Gorp, M., Denecker, G., Demeulemeester, J., Kalai, M., Declercq, W., Saelens, X., and Vandenabeele, P. (2005). A novel caspase-2 complex containing TRAF2 and RIP1. *J. Biol. Chem.* **280**, 6923–6932.
- Lee, J. H., and Paull, T. T. (2005). ATM activation by DNA double-strand breaks through the Mre11-Rad50-Nbs1 complex. *Science* **308**, 551–554.
- Lee, J. H., and Paull, T. T. (2007). Activation and regulation of ATM kinase activity in response to DNA double-strand breaks. *Oncogene* **26**, 7741–7748.
- Ljungman, M. (2005). Activation of DNA damage signaling. *Mutat. Res.* **577**, 203–216.
- Lu, C., Shi, Y., Wang, Z., Song, Z., Zhu, M., Cai, Q., and Chen, T. (2008). Serum starvation induces H2AX phosphorylation to regulate apoptosis via p38 MAPK pathway. *FEBS Lett.* **582**, 2703–2708.
- Lu, C., Zhu, F., Cho, Y. Y., Tang, F., Zykova, T., Ma, W. Y., Bode, A. M., and Dong, Z. (2006). Cell apoptosis: requirement of H2AX in DNA ladder formation, but not for the activation of caspase-3. *Mol. Cell.* **23**, 121–132.
- Marti, T. M., Hefner, E., Feeney, L., Natale, V., and Cleaver, J. E. (2006). H2AX phosphorylation within the G1 phase after UV irradiation depends on nucleotide excision repair and not DNA double-strand breaks. *Proc. Natl. Acad. Sci.* **103**, 9891–9896.
- Mattson, M. P., and Furukawa, K. (1997). Anti-apoptotic actions of cycloheximide: blockade of programmed cell death or induction of programmed cell life? *Apoptosis* **2**, 257–264.
- McLaughlin, C. S., Vaughan, M. H., Campbell, I. M., Wei, C. M., Stafford, M. E., and Hansen, B. S. (1977). Inhibition of protein synthesis by trichothecenes. In *Mycotoxins in Human and Animal Health* (J. V. Rodricks, C. W. Hesseltine, and M. A. Mehlman, Eds.), pp. 261–284. Pathotox Publications, Park Forest South, IL.
- Nagase, M., Alam, M. M., Tsushima, A., Yoshizawa, T., and Sakato, N. (2001). Apoptosis induction by T-2 toxin: activation of caspase-9, caspase-3, and DFF-40/CAD through cytosolic release of cytochrome c in HL-60 cells. *Biosci. Biotechnol. Biochem.* **65**, 1741–1747.
- Nagase, M., Shiota, T., Tsushima, A., Alam, M. M., Fukuoka, S., Yoshizawa, T., and Sakato, N. (2002). Molecular mechanism of satratoxin-induced apoptosis in HL-60 cells: activation of caspase-8 and caspase-9 is involved in activation of caspase-3. *Immunol. Lett.* **84**, 23–27.
- Nielsen, K. F., Huttunen, K., Hyvärinen, A., Andersen, B., Jarvis, B. B., and Hirvonen, M. R. (2002). Metabolite profiles of Stachybotrys isolates from water-damaged buildings and their induction of inflammatory mediators and cytotoxicity in macrophages. *Mycopathologia* **154**, 201–205.
- Olmo, N., Turnay, J., Gonzalez de Buitrago, G., Lopez de Silanes, I., Gavilanes, J. G., and Lizarbe, M. A. (2001). Cytotoxic mechanism of the ribotoxin alpha-sarcosine. Induction of cell death via apoptosis. *Eur. J. Biochem.* **268**, 2113–2123.
- Pestka, J. J., Yike, I., Dearborn, D. G., Ward, M. D., and Harkema, J. R. (2008). Stachybotrys chartarum, trichothecene mycotoxins, and damp building-related illness: new insights into a public health enigma. *Toxicol. Sci.* **104**, 4–26.
- Rogakou, E. P., Boon, C., Redon, C., and Bonner, W. M. (1999). Megabase chromatin domains involved in DNA double-strand breaks in vivo. *J. Cell. Biol.* **146**, 905–916.
- Roos, W. P., and Kaina, B. (2006). DNA damage-induced cell death by apoptosis. *Trends Mol. Med.* **12**, 440–450.
- Ruotsalainen, M., Hirvonen, M. R., Hyvärinen, A., Meklin, J., Savolainen, K., and Nevalainen, A. (1998). Cytotoxicity, production of reactive oxygen species and cytokines induced by different strains of Stachybotrys sp. from moldy buildings in RAW264.7 macrophages. *Environ. Toxicol. Pharmacol.* **6**, 193–199.
- Samson, R. A., Hoekstra, E. S., and Frisvad, J. C. (2004). In *Introduction to Food- and Airborne Fungi*, 7th ed. Centraalbureau voor Schimmelfungi, Utrecht, The Netherlands.
- Shifrin, V. I., and Anderson, P. (1999). Trichothecene mycotoxins trigger a ribotoxic stress response that activates c-Jun N-terminal kinase and p38 mitogen activated protein kinase and induces apoptosis. *J. Biol. Chem.* **274**, 13985–13992.
- Smart, D. J., Halicka, H. D., Schmuck, G., Traganos, F., Darzynkiewicz, Z., and Williams, G. M. (2008). Assessment of DNA double-strand breaks and γH2AX induced by the topoisomerase II poisons etoposide and mitoxantrone. *Mutat. Res.* **641**, 43–47.
- Solhaug, A., Refsnes, M., Låg, M., Schwarze, P. E., Husøy, T., and Holme, J. A. (2004). Polycyclic aromatic hydrocarbons induce both apoptotic and anti-apoptotic signals in Hepa1c17 cells. *Carcinogenesis* **25**, 809–819.
- Sugimoto, K., Toyoshima, H., Sakai, R., Miyagawa, K., Hagiwara, K., Ishikawa, F., Takaku, F., Yazaki, Y., and Hirai, H. (1992). Frequent mutations in the p53 gene in human myeloid leukemia cell lines. *Blood* **79**, 2378–2383.
- Tanaka, T., Huang, X., Halicka, H. D., Zhao, H., Traganos, F., Albino, A. P., Dai, W., and Darzynkiewicz, Z. (2007a). Cytometry of ATM activation and

- histone H2AX phosphorylation to estimate extent of DNA. *Cytometry A* **71**, 648–661.
- Tanaka, T., Huang, X., Jorgensen, E., Gietl, D., Traganos, F., Darzynkiewicz, Z., and Albino, A. P. (2007b). ATM activation accompanies histone H2AX phosphorylation in A549 cells upon exposure to tobacco smoke. *BMC Cell Biol.* **8**, 26.
- Towbin, H., Staehelin, T., and Gordon, J. (1979). Electrophoretic transfer of proteins from polyacrylamide gels to nitrocellulose sheets: procedure and some applications. *Proc. Natl. Acad. Sci. U.S.A.* **76**, 4350–4354.
- Versilovskis, A., and De Saeger, S. (2010). Sterigmatocystin: occurrence in foodstuffs and analytical methods—an overview. *Mol. Nutr. Food Res.* **54**, 136–147.
- Wang, J. S., and Groopman, J. D. (1999). DNA damage by mycotoxins. *Mutat. Res.* **424**, 167–181.
- Wang, H., and Joseph, J. A. (1999). Quantifying cellular oxidative stress by dichlorofluorescein assay using microplate reader. *Free Radic. Biol. Med.* **27**, 612–616.
- Wang, H., and Yadav, J. S. (2006). DNA damage, redox changes, and associated stress-inducible signaling events underlying the apoptosis and cytotoxicity in murine alveolar macrophage cell line MH-S by methanol-extracted *Stachybotrys chartarum* toxins. *Toxicol. Appl. Pharmacol.* **214**, 297–308.
- Yang, G.-H., Jarvis, B. B., Chung, Y.-J., and Pestka, J. J. (2000). Apoptosis induction by the satratoxins and other trichothecene mycotoxins: relationship to ERK, p38 MAPK, and SAPK/JNK activation. *Toxicol. Appl. Pharmacol.* **164**, 149–160.
- Yang, X., and Chan, C. (2009). Repression of PKR mediates palmitate-induced apoptosis in HepG2 cells through Bcl-2. *Cell Res.* **19**, 469–486.
- Yike, I., Rand, T., and Dearborn, D. G. (2007). The role of fungal proteinases in pathophysiology of *Stachybotrys chartarum*. *Mycopathologia* **164**, 171–181. Epub 2007 July 3.
- Zarubin, T., and Han, J. (2005). Activation and signaling of the p38 MAP kinase pathway. *Cell Res.* **15**, 11–18.
- Zhou, H.-R., Islam, Z., and Pestka, J. J. (2005a). Induction of competing apoptotic and survival signaling pathways in the macrophage by the ribotoxic trichothecene deoxynivalenol. *Toxicol. Sci.* **87**, 113–122.
- Zhou, H.-R., Jia, Q., and Pestka, J. J. (2005b). Ribotoxic stress response to the trichothecene deoxynivalenol in the macrophage involves the Src family kinase Hck. *Toxicol. Sci.* **85**, 916–926.
- Zhou, H.-R., Lau, A. S., and Pestka, J. J. (2003). Role of double-stranded RNA-activated protein kinase R (PKR) in deoxynivalenol-induced ribotoxic stress response. *Toxicol. Sci.* **74**, 335–344.